

Cite this: *Chem. Sci.*, 2022, 13, 12791

All publication charges for this article have been paid for by the Royal Society of Chemistry

Received 16th August 2022  
Accepted 13th October 2022

DOI: 10.1039/d2sc04574e

rsc.li/chemical-science

# Insight into *ortho*-boronoaldehyde conjugation via a FRET-based reporter assay†

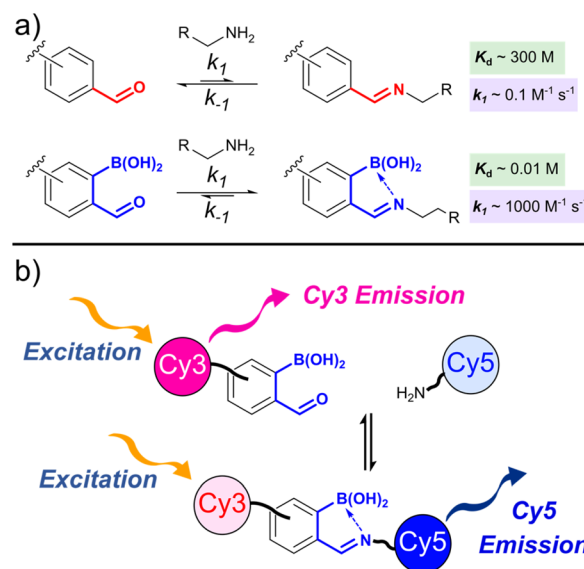
Nicholas C. Rose,<sup>ab</sup> Anaïs V. Sanchez,<sup>ab</sup> Eve F. Tipple,<sup>ab</sup> Jason M. Lynam<sup>ab</sup> and Christopher D. Spicer<sup>ab\*</sup>

*Ortho*-boronoaldehydes react with amine-based nucleophiles with dramatically increased rates and product stabilities, relative to unfunctionalised benzaldehydes, leading to exciting applications across biological and material chemistry. We have developed a novel Förster resonance energy transfer (FRET)-based assay to provide key new insights into the reactivity of these boronoaldehydes, allowing us to track conjugation with unprecedented sensitivity and accuracy under standardised conditions. Our results highlight the key role played by reaction pH, buffer additives, and boronoaldehyde structure in controlling conjugation speed and stability, providing design criteria for further innovations and applications in the field.

Reactions between *ortho*-boronoaldehydes (oBAs) and amine-based nucleophiles have emerged as powerful tools for bio-conjugation and materials chemistry over the last decade, due to a combination of rapid reaction rates and tunable product stability. The *ortho*-boronoimines, and related derivatives (collectively oBIDs), that form have shown high potential in drug delivery,<sup>1</sup> *in vivo* labelling,<sup>2</sup> and responsive materials.<sup>3</sup> To allow further evolution of these technologies and drive innovative new applications, there is a pressing need for increased understanding of the formation of oBIDs and their responsive behaviour. In this work, we deliver a sensitive and versatile platform to realise such understanding, through a Förster resonance energy transfer (FRET) reporter assay of oBID formation. This assay allows us to probe the rapid kinetics of oBID formation in detail, under complex and biomedically relevant conditions.

The *ortho*-boronic acid accelerates the rate of oBID formation ( $k_1$ ), relative to unfunctionalised benzaldehyde, by both activating the aldehyde to nucleophilic attack and accelerating the rate-determining dehydration step. Though the rate of hydrolysis ( $k_{-1}$ ) is also accelerated, stabilising B–N interactions lead to a significant overall shift in equilibrium towards product formation (decrease in dissociation constant,  $K_d$ ). For example, while benzaldehyde reacts with alkyl amines with  $k_1 \sim 0.1 \text{ M}^{-1} \text{ s}^{-1}$  and  $K_d \sim 300 \text{ M}$ ,<sup>4</sup> the *ortho*-borono analogue *ortho*-formylphenylboronic acid (FBPA) forms analogous iminoboronates with a  $k_1 \sim 1000 \text{ M}^{-1} \text{ s}^{-1}$  and  $K_d \sim 10 \text{ mM}$  (Fig. 1a).<sup>5</sup> This

5-order of magnitude increase in reaction rate, and 4-order of magnitude decrease in dissociation constant, typifies the unique reactivity of oBAs.



- Monitor rapid reactions at **low concentrations**
- Sensitive measure of **conjugation**, not structure
- Tolerant of **diverse conditions** and media
- **Standardised platform** for comparison

Fig. 1 (a) Comparison of benzaldehyde and *ortho*-boronoaldehyde reactivity, with the *ortho*-borono group both accelerating and stabilising imine formation; (b) schematic overview of the FRET platform developed in this work, allowing sensitive monitoring of rapid oBID formation ( $k_1 > 10^5 \text{ M}^{-1} \text{ s}^{-1}$ ).

<sup>a</sup>Department of Chemistry, University of York, Heslington, YO10 5DD, UK. E-mail: chris.spicer@york.ac.uk

<sup>b</sup>York Biomedical Research Institute, University of York, Heslington, YO10 5DD, UK

† Electronic supplementary information (ESI) available: The supporting information contains all experimental details, including reagent synthesis, FRET measurements, and studies of reversibility. See DOI: <https://doi.org/10.1039/d2sc04574e>

Through variation of the *o*BA and nucleophile coupling partners,  $K_{\text{ds}}$  spanning  $10^{-2}$ – $10^{-9}$  M have been reported.<sup>6</sup> When coupled with high biocompatibility and potential for stimuli-responsive behaviour, this tunability greatly enhances the potential for biomedical applications of *o*BIDs. Despite this potential, much of our understanding of *o*BID chemistry comes from simple, unsubstituted model compounds such as FPBA, which poorly reflect the stereo-electronic characteristics of the functionalised *o*BA's necessary for translational applications.

Moreover, much of this understanding is pieced together from a large number of independent studies, performed and analysed under varying conditions, making comparison challenging. This is particularly important given the highly dynamic nature of *o*BID linkages, leading to a high sensitivity to environmental conditions and choice of analytical technique. Ultimately, this leads to significant discrepancies in reported rates of formation and stabilities of *o*BIDs, due to subtle differences in substrate choice, reaction conditions, or analysis method.<sup>7,8</sup>

To address this, we herein describe a versatile and sensitive FRET-assay for studying *o*BID formation, stability, and cleavage. This assay is highly tolerant of environmental conditions, allowing us to provide critical new insights into the effects of pH, additives, media, and *o*BA structure on conjugation. We therefore anticipate that this assay will find future use for the high-throughput screening of novel *o*BIDs and their stimuli-responsive behaviour.

## Results and discussion

### Platform design

To develop a platform for studying *o*BID chemistry, we took three key considerations into account:

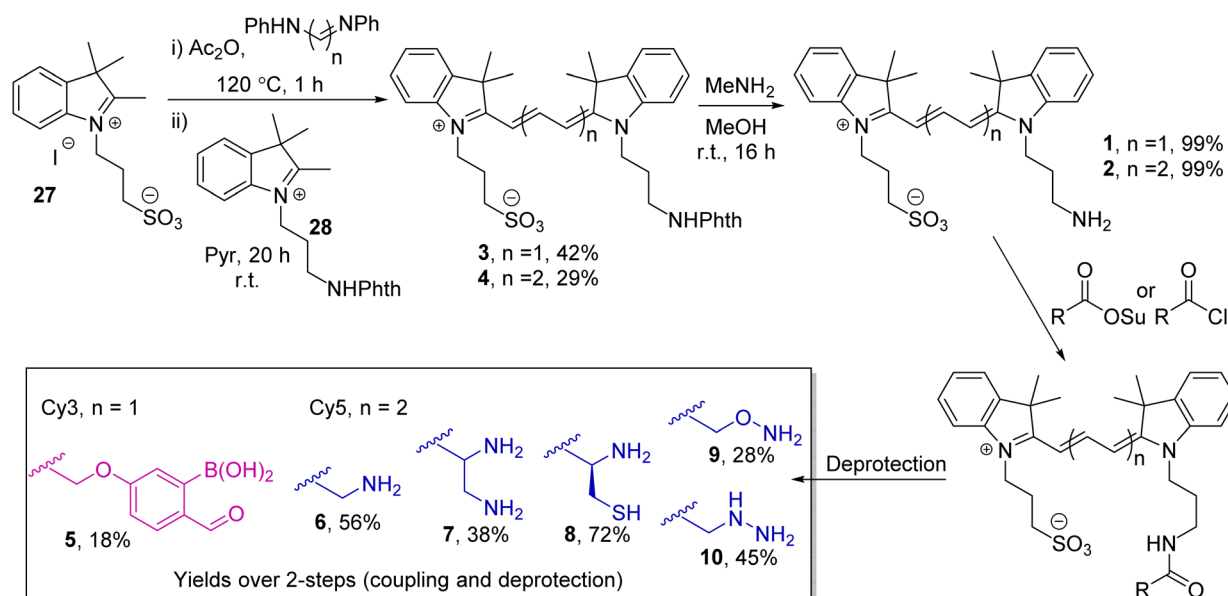
(i) The platform should be operational at low concentrations. Many *o*BIDs form with  $k_1 > 10^3 \text{ M}^{-1} \text{ s}^{-1}$ , and at the substrate

concentrations required for UV-vis/NMR analysis reactions are complete prior to the first measurements, preventing accurate quantification.<sup>9–11</sup> Sensitive detection of *o*BID formation at low concentrations is therefore essential to allow a suitable number of time points to be recorded before equilibrium is reached;

(ii) The platform should function across a broad range of reaction conditions representative of the end applications, including the presence of complex additives, allowing us to study *o*BID formation under conditions relevant to biological applications;

And (iii) a readout of conjugation, rather than structure, should be provided. Following conjugation of an *o*BA and nucleophile, the *o*BID formed remains highly dynamic. Often, complex mixtures of rapidly interchanging species exist in equilibrium, in a manner that is highly sensitive to environmental conditions (*e.g.* pH dependent equilibrium between *ortho*-boronohydrazones and diazaborines;<sup>12</sup> diastereomeric mixtures formed during thiazolidino boronate formation<sup>8</sup>). By focussing on conjugation, we would be able to gain an overall view of all species that contribute positively to *o*BID formation, which would not be provided by focussing on the formation of specific structures. UV-vis and NMR studies are again poorly suited to providing such an overview.

We reasoned that a FRET-based reporter system would fulfil these criteria (Fig. 1b).<sup>13</sup> Upon conjugation of complementary dyes bearing either *o*BA or nucleophile reactive handles, the proximity of the dyes would allow energy transfer to take place under donor excitation. The donor:acceptor emission ratio (FRET ratio) would then directly correlate to reaction conversion, and would be largely independent of *o*BID structure. Notably, Schmidt *et al.* previously exploited a fluorescence quenching assay to monitor borono-oxime formation, but such experiments can be prone to interference from environmental conditions. In contrast, the ratiometric nature of FRET



Scheme 1 Synthesis of *o*BA-functionalised Cy3 dye 5 and nucleophile-functionalised Cy5 dyes 6–10.



minimises such complications, and provides an extra level of robustness to kinetic measurements.<sup>14</sup>

The cyanine dyes Cy3 and Cy5 were chosen as a suitable FRET pair due to their chemical-, thermal-, and photo-stability, emission across a wide pH range, and known ability to undergo energy transfer.<sup>15</sup> Due to the strong distance dependence of FRET ( $1/r^6$ ), we aimed to minimise the linker length from the dyes to the *o*BA/nucleophile functional handles, leading us to synthesise novel amino-cyanines **1** and **2** (Scheme 1). These derivatives, bearing a pendant sulfonate group that enhanced water solubility without affecting fluorescence,<sup>15</sup> could be easily derivatised *via* amide coupling. Phthalimide protection of the amine (**3** and **4**) was required due to the harsh conditions needed for synthesis of the dye cores. Though traditional hydrazinolysis of the phthalimide was found to be problematic, due to the reaction of hydrazine with the conjugated backbone of Cy5, deprotection could be successfully achieved with high concentrations of methylamine to deliver **1** and **2** on a gram scale.

With the parent dyes in hand, they were functionalised with reactive handles for *o*BID formation. A 2-borono-4-alkoxy-benzaldehyde handle (**5**) was chosen as a representative *o*BA for attachment to Cy3 **1**. This choice was based on the ease with which **5** could be synthesised, relative to other *o*BA analogues, and therefore its position as a widely used functional *o*BA within the community.<sup>16–18</sup> However, as discussed later, this choice of *o*BA plays a role in dictating conjugation rate and stability, and therefore has significant implications.

As nucleophiles, Cy5 analogues **6–10** were synthesised to represent the most common reagents for *o*BID formation. These analogues encompass the archetypal amine nucleophile (**6**) associated with iminoboronate formation (**11**),<sup>19</sup> 1,2-diamine (**7**)<sup>18</sup> and 1,2-aminothiol (**8**)<sup>8</sup> based nucleophiles which form cyclic imidazolidino- (IzB, **12**) and thiazolidino- (TzB, **13**) boronates respectively, and the ' $\alpha$ -effect' hydroxylamine (**9**)<sup>14</sup> and hydrazine (**10**)<sup>20</sup> handles that react to form stabilised oximes (**14**) and hydrazones/diazoborines (DAB, **15**). A consistent linker structure was used to minimise any distance-dependent changes in FRET efficiency.

### Preliminary platform validation

*o*BID formation was initially screened in a 96-well format under pseudo-first order conditions, to allow optimal timeframes for reaction monitoring to be established. Significant drops in Cy3 emission (580 nm) were observed for mixtures of Cy3-*o*BA **5** (5  $\mu$ M) and nucleophiles **7–11** (50  $\mu$ M) over a 30 minutes timeframe, with amine **6** leading to little change (See ESI Fig. S1†). Importantly, control reactions between **5** and nucleophiles that were not functionalised with the Cy5 acceptor, did not lead to a change in Cy3 emission (See ESI Fig. S2†). This confirmed that energy transfer was taking place between the two dyes specifically upon conjugation, and ruled out non-radiative quenching by the *o*BID. Similarly, no drop in emission was seen for control reactions using Cy3 substrates lacking either the boronic acid or aldehyde functional groups, confirming the importance of B–N stabilisation. Though benzaldehyde can form non-stabilised

thiazolidines, oximes, and hydrazones under these conditions, reactions are slow at neutral pH in the absence of catalysts ( $k_1 < 0.01 \text{ M}^{-1} \text{ s}^{-1}$ ) and therefore would not be expected to form over the timeframes of these studies.<sup>21,22</sup> Cumulatively, these experiments validate the platform design.

### *o*BID formation at pH 7.4

Following these preliminary studies, we went on to study the formation of **11–15** under second-order conditions. Cy3-*o*BA donor **5** was mixed with nucleophiles **6–10** at a concentration of 2.5  $\mu$ M in phosphate buffered saline (pH 7.4, experiments run in triplicate, Fig. 2a). Emission spectra (520–700 nm) following Cy3 excitation were then recorded every 15 seconds over a period of 25 min. To correlate Cy3 : Cy5 emission ratios to conversions, reactions using an acetyl-capped Cy5-amine **16** (negative '0% conversion

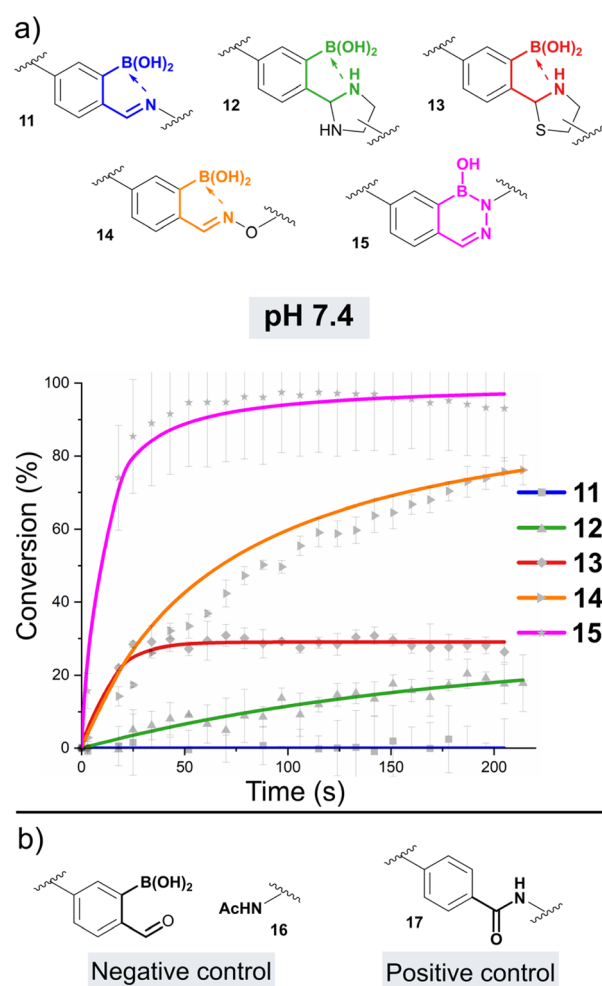


Fig. 2 (a) Plot of reaction conversion against time for the formation of *o*BIDs **11–15** from Cy3-*o*BA **5** and the relevant Cy5-nucleophile. Reactions were run at a concentration of 2.5  $\mu$ M under second-order conditions at pH 7.4. Fits are based on second-order irreversible (**14**, **15**) or reversible models (**11–13**), with errors based on the standard deviation of experiments run in triplicate; (b) control substrates used to provide reference measurements for the calculation of conversions. Nb. data for **11** tracks the baseline (0% conversion) across all time points.



conjugation' control) and a covalently linked Cy3-Cy5 pair **17** (positive '100% conjugation' control) were used as references (Fig. 2b and Table 1, see ESI Section 9† for details of data processing).

As expected given reports of  $K_d \sim 10$  mM, iminoboronate **11** was not found to form to an appreciable extent at the low concentrations of these experiments.<sup>6</sup> However, for the formation of IzB **12** and TzB **13** the data was found to fit a reversible second-order kinetic model, allowing us to extrapolate  $k_1$  and  $k_{-1}$ , and thus calculate  $K_d$ .<sup>23</sup> Interestingly, though the overall position of equilibrium for each reaction was similar ( $K_d \sim 4$ – $5$   $\mu$ M), IzB was found to form at an order of magnitude higher rate ( $\sim 9900$   $\text{M}^{-1} \text{s}^{-1}$  vs.  $610$   $\text{M}^{-1} \text{s}^{-1}$ ), highlighting thiol cyclisation as rate-limiting for the formation of a stable conjugate. Though our results are in line with previous reports on TzB formation,<sup>5</sup> the rate of IzB formation was found to be accelerated by a factor of 10 relative to literature precedent.<sup>18</sup> This difference can be attributed to the use of a functionalised 2-borono-4-alkoxy-benzaldehyde handle within our studies, in contrast to the use of FPBA models in the previous reports. This result therefore highlights the critical importance of studying derivatised oBIDs which more accurately reflect the substrates used in real-world applications. Moreover, our measurements were insensitive to the mixtures of diastereomers which complicate NMR analysis of IzB and TzB formation, providing further benefit over previous analyses.<sup>18,22</sup>

The formations of oxime **14** and hydrazone/DAB **15** were found to fit a second-order irreversible model, and so  $k_1$  was calculated from plots of inverse reagent concentration against time. Due to the fast kinetics with which **15** was formed, reactions were performed at high dilutions (750 nM) to provide sufficient data points within the linear region of the plot (See ESI Fig. S3†). Attempts to cleave **14** or **15** using an excess of a competitive nucleophile were unsuccessful, due to slow side-reactions with the conjugated framework of the dyes which became significant over the long timeframes of the

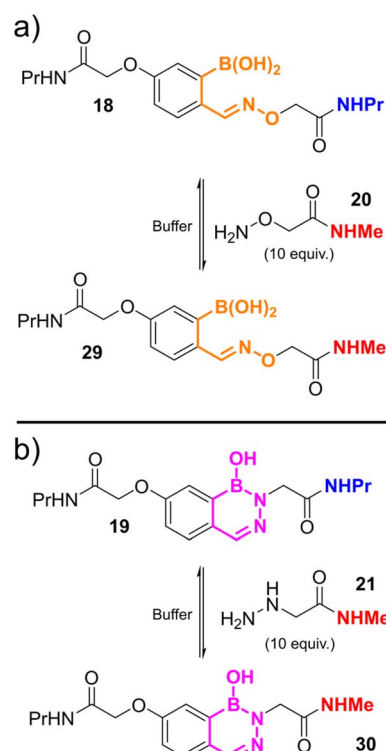
equilibration. We therefore monitored the equilibration between propyl-amine functionalised oxime **18** or DAB **19** and an excess of a competitive nucleophile (**20** or **21**) via liquid chromatography analysis, allowing us to determine the rate of hydroxylamine/hydrazine exchange and thus calculate  $k_{-1}$  and  $K_d$  (Scheme 2, see ESI Fig. S4† for data).

The rate of oxime formation and dissociation constant ( $k_1 \sim 5000$   $\text{M}^{-1} \text{s}^{-1}$ ;  $K_d \sim 10$  nM) is in line with previous reports by Schmidt *et al.* ( $k_1 \sim 11\,000$   $\text{M}^{-1} \text{s}^{-1}$ ;  $K_d \sim 25$  nM). Interestingly, this previous work studied the reactivity of 2-borono-5-alkoxy benzaldehydes, in contrast to the 4-alkoxy analogues used in this work, again highlighting the contributions of stereo-electronic arrangements to oBA reactivity.<sup>14</sup>

The reactivity of hydrazines with FPBA has been studied extensively by the Bane and Gillingham groups. They have shown that following the formation of an intermediate hydrazone, a second intramolecular cyclisation and dehydration step results in the eventual formation of an aromatic DAB at neutral pH. Though the rates of DAB formation have been determined ( $\sim 0.01$   $\text{s}^{-1}$ ), previous studies have had insufficient kinetic resolution to provide insight into the initial hydrazone formation.<sup>10,12,20</sup> Our results indicate that this step is remarkably rapid, with  $k_1 \sim 10^5$   $\text{M}^{-1} \text{s}^{-1}$ . Within the timeframe of our FRET experiments, it is unlikely that DAB formation makes a significant contribution, but would not be expected to significantly affect our FRET results, which report on conjugation not

Table 1 Tabulated dissociation ( $K_d$ ) and rate ( $k_1$ ,  $k_{-1}$ ) constants for the formation of oBIDs **11**–**15**

	pH	$k_1/\text{M}^{-1} \text{s}^{-1}$	$k_{-1}/\text{s}^{-1}$	$K_d$
<b>11</b>	6	—	—	—
<b>12</b>	6	—	—	—
<b>13</b>	6	$250 \pm 3$	$1.13 \pm 0.04 \times 10^{-3}$	4.5 $\mu$ M
<b>14</b>	6	$3034 \pm 27$	$6.04 \pm 1.08 \times 10^{-5}$	19 nM
<b>15</b>	6	$22\,920 \pm 839$	$8.07 \pm 0.29 \times 10^{-6}$	352 pM
<b>11</b>	7.4	—	—	—
<b>12</b>	7.4	$9882 \pm 978$	$4.02 \pm 0.45 \times 10^{-2}$	4.3 $\mu$ M
<b>13</b>	7.4	$613 \pm 16$	$3.01 \pm 0.11 \times 10^{-3}$	4.9 $\mu$ M
<b>14</b>	7.4	$4370 \pm 164$	$5.61 \pm 1.28 \times 10^{-5}$	12 nM
<b>15</b>	7.4	$169\,030 \pm 6962$	$2.60 \pm 0.55 \times 10^{-6}$	15 pM
<b>11</b>	8	—	—	—
<b>12</b>	8	$17\,521 \pm 1211$	$2.72 \times 10^{-2}$	1.5 $\mu$ M
<b>13</b>	8	$21\,261 \pm 591$	$1.22 \times 10^{-3}$	57 nM
<b>14</b>	8	$1528 \pm 10$	$3.56 \pm 0.11 \times 10^{-4}$	233 nM
<b>15</b>	8	$37\,471 \pm 1238$	$8.05 \pm 0.26 \times 10^{-6}$	215 pM
<b>14</b>	4	$1517 \pm 81$	$5.23 \pm 0.56 \times 10^{-5}$	34 nM
<b>15</b>	4	$876 \pm 163$	$3.36 \pm 0.70 \times 10^{-2}$	38 $\mu$ M



Scheme 2 Equilibration of (a) propylamine-oxime **18** with and excess of methylamine-functionalised hydroxylamine **20**; and (b) propylamine-DAB **19** with an excess of methylamine-functionalised hydrazine **21**; allowing  $k_{-1}$  to be calculated over extended periods of time via LC-MS analysis.





structure, regardless. This result again highlights the benefit of analysing all conjugated products collectively, rather than individual species which may otherwise be undergoing exchange or serving as intermediates towards an eventual thermodynamic product. Equilibration studies over the course of 1 week indicated the reaction remained dynamic, with **19** undergoing hydrolysis with a rate of  $\sim 10^{-6} \text{ s}^{-1}$  leading to a  $K_d$  for hydrazone/DAB formation of  $\sim 10 \text{ pM}$  (see ESI Fig. S4†). To the best of our knowledge, this represents the lowest  $K_d$  recorded for a dynamic oBID to date, in contrast to the nopoldiol-stabilised thiosemicarbazone reagents developed by the Hall group which show no reversibility.<sup>24</sup>

### pH-dependent oBID formation

We next went on to study the pH dependence of oBID formation (Fig. 3 and Table 1, see ESI Fig. S5† for data arranged by nucleophile rather than pH). The formation of IzB **12** was accelerated at pH 8 ( $k_1 \sim 17\,500 \text{ M}^{-1} \text{ s}^{-1}$ ), with a corresponding small increase in stability, but at pH 6 no conversion was observed. Accounting for error and noise within our calculations, this means  $K_d > 45 \text{ }\mu\text{M}$  for IzB formation under such conditions. Notably, Li *et al.* previously reported that the carboxylic acid of diaminopropionic acid was able to cyclise to form a mixed boron-carbon anhydride structure which was favoured at pH 6 and stabilised IzB formation. However, when the 1,2-diamine is conjugated to a functional cargo, as in our system, no such interactions are possible demonstrating the importance of studying models relevant to functional applications.<sup>18</sup>

A similar increase in reaction was observed for the formation of TzB **13** at pH 8. In contrast to the results obtained at pH 7.4, TzB formation was actually faster than IzB formation at this pH ( $k_1 \sim 37\,000 \text{ M}^{-1} \text{ s}^{-1}$  vs.  $21\,000 \text{ M}^{-1} \text{ s}^{-1}$ ), presumably due to the accelerated cyclisation of the deprotonated thiolate that can form at higher pH. The stability of the TzB was also increased by 2-orders of magnitude ( $K_d \sim 50 \text{ nM}$ ). At pH 6, the rate of formation and stability of **13** was comparable to the results obtained at pH 7.4, lending further support to the hypothesis that the protonation state of the thiol plays a key role in TzB formation.

For the formation of oxime **14**, pH 7.4 was found to provide optimal stability within the conditions tested ( $K_d \sim 10 \text{ nM}$ ). At pH 6 or 8,  $k_1$  was reduced slightly, but contributions from accelerated oxime hydrolysis to  $K_d$  were far more significant leading to  $K_d$ s  $\sim 20 \text{ nM}$  and  $200 \text{ nM}$  at pH 6 and 8 respectively. These results are in line with recent work by Han and Domaille,<sup>25</sup> as well as a prior study by Schmidt *et al.*,<sup>14</sup> showing that borono-oxime stability is highly pH dependent. Interestingly, at pH 4  $K_d \sim 34 \text{ nM}$ , indicating that acidic pH did not have a large effect on borono-oxime stability.

At both pH 6 and 8, the rate of reaction between oBA **5** and hydrazine **10** was reduced relative to the reaction at pH 7.4, with a corresponding increase in  $k_{-1}$  leading to an overall increase in  $K_d$  from  $\sim 10 \text{ pM}$  at pH 7.4 to  $\sim 300 \text{ pM}$  and  $\sim 200 \text{ pM}$  at pH 6 and 8 respectively. Overall, the reactions were still found to proceed very rapidly at both pHs though, with  $k_1$   $22\,000$ – $37\,000 \text{ M}^{-1} \text{ s}^{-1}$

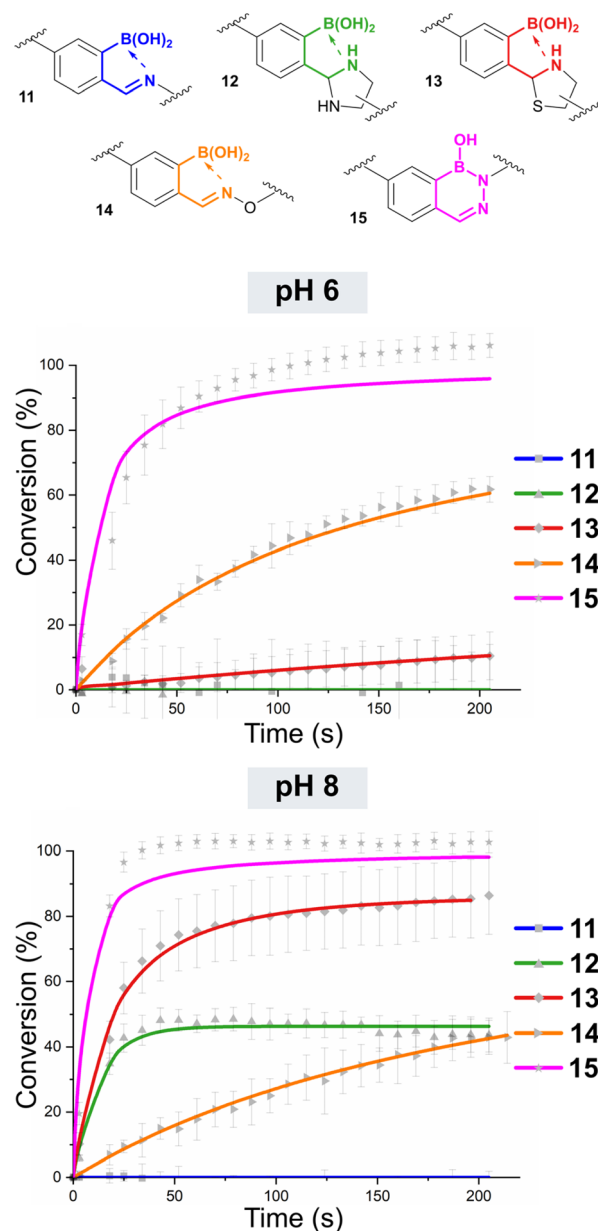


Fig. 3 Plot of reaction conversion against time for the formation of oBIDs **11**–**15** from Cy3-oBA **5** and the relevant Cy5-nucleophile. Reactions were run at a concentration of  $2.5 \text{ }\mu\text{M}$  under second-order conditions at pH 6 or 8. Fits are based on second-order irreversible (**15**) or reversible models (**11**–**14**), with errors based on the standard deviation of experiments run in triplicate. Nb. data for **11** tracks the baseline (0% conversion) across all time points.

necessitating measurements at lowered concentrations ( $750 \text{ nM}$ ) to allow sufficient data points for analysis. At pH 4, the rate of formation of **15** was greatly decreased ( $\sim 850 \text{ M}^{-1} \text{ s}^{-1}$ ), with conjugate stability showing an even more dramatic 6-orders of magnitude drop ( $K_d \sim 40 \text{ }\mu\text{M}$ ). It is noteworthy that at pH 4 Gu *et al.* reported that for the reaction of oBAs with related hydrazides, the open chain hydrazone oBID is dominant over the cyclic DAB.<sup>12</sup> However, we found that the products formed from the hydrazine nucleophiles used in this study existed solely as the ring-closed DAB, with no evidence of the ring-open

hydrazone by NMR, even at pH 4 (see ESI Section 11†). A switch between ring-closed and ring-open structure is therefore not responsible for the altered stability at lower pH.

### Reaction additives

The ability to study *o*BID formation in the presence of additives, which would otherwise complicate absorbance measurements, is a major benefit of our FRET-based approach. Monosaccharides and more complex sugars are present at high concentrations in biological settings (glucose  $\sim 5$  mM in blood) and are known to dynamically complex boronic acids, and are therefore likely to play a significant role in *o*BID chemistry. In a number of reports it has been shown that pre-formed *o*BIDs are relatively stable to the addition of both glucose ( $K_d \sim 10$  mM with phenylboronic acid) and fructose ( $K_d \sim 500$   $\mu$ M), but less is known about how these sugars affect *o*BID formation.<sup>26</sup> The formations of **14** and **15** were therefore monitored in PBS containing 100 mM of either monosaccharide (Table 2, see ESI Fig. S6†). In all cases, rates of conjugation were found to be slowed, with fructose having a more significant influence in accordance with its higher boronic acid binding ability ( $\sim \times 10$  reduction in  $k_1$  for both hydroxylamine and hydrazine reactivity).

In the case of hydrazones/DABs, the decrease in  $k_1$  led to an overall small increase in  $K_d$  (50–150 pM, vs. 15 pM in the absence of additives), despite there being no effect of either sugar on  $k_{-1}$ . This may suggest that monosaccharides do not complex hydrazones/DABs once formed, nor does pre-complexation lead to a stable tri-component complex, as such scenarios would lead to differing  $k_{-1}$  values across the three samples. In contrast, the stability of oxime **14** was significantly decreased ( $K_d \sim 100$ –500 nM), in contrast to previous reports that suggest minimal influence of sugar additives on the stability of pre-formed oximes.<sup>14</sup> There are two possible origins for this effect: (i) The increased sensitivity of our platform may have given insight into reversibility that was not previously observed due to the use of high reagent concentrations; or (ii) The presence of glucose/fructose during the reaction altered the structure of the product formed. For example, it is possible that sugar complexation after oxime formation is no longer possible/favoured, and so tests of stability could give contrasting results to reactions that study formation in the presence of the additive. To investigate this, oxime **18** or DAB **19** were incubated at pH 7.4

with either glucose or fructose at a concentration of 9 mM and binding was assessed *via* NMR. In all cases, no binding was observed, suggesting sugar complexation is not a major contributing factor to oxime or DAB stability at concentrations relevant to this study (see ESI Section 12†). Further investigations are currently ongoing in our lab to study the interplay between *o*BA-sugar binding and reaction kinetics, and to elucidate the effects of other relevant additives on *o*BID formation, structure, and stability, exploiting the platform reported here.

To further demonstrate the benefits of our approach, we next studied the formation and stability of oxime and hydrazone/DAB constructs in serum (Table 2, see ESI Fig. S6†). Understanding *o*BID chemistry in this environment is essential for future *in vivo* applications, particularly for potential within drug delivery to be realised. However, studying conjugation chemistry within serum is highly challenging due to its complex composition. The limited number of previous studies into *o*BID formation have relied on high concentrations of reagents that may not truly reflect the end application.<sup>11,14</sup> In contrast, as background fluorescence within the 520–700 nm window is minimal and can be accounted for, FRET provides us with an ideal means to monitor *o*BID formation in serum at low  $\mu$ M concentrations.

The rate of oxime formation was slowed significantly in the presence of 10% bovine serum ( $k_1 \sim 60$   $\text{M}^{-1} \text{s}^{-1}$  vs. 4000  $\text{M}^{-1} \text{s}^{-1}$  in PBS), and the conjugates were also found to be highly dynamic, with a  $K_d \sim 15$   $\mu$ M being observed. The decrease in reaction rate was even more significant for hydrazine **15**, with a three order of magnitude reduction in  $k_1$  being recorded ( $\sim 150$   $\text{M}^{-1} \text{s}^{-1}$ ). Furthermore, conjugation was also found to be dynamic with a  $K_d \sim 20$   $\mu$ M. Since the rate of DAB formation is significantly slower than initial hydrazone formation, this data may indicate that this intermediate species is dynamic in the presence of serum, with implications for *o*BID formation in complex medias. In contrast, when DAB **15** was pre-formed in PBS prior to dilution in 10% serum, the FRET ratio was found to stay unchanged over a period of 25 min (see ESI Fig. S7†). This supports previous reports that DABs are stable in serum, with exciting opportunities for future *in vivo* applications. Interestingly, oximes pre-formed in PBS were also observed to undergo minimal change in FRET ratio upon addition of 10% serum, pointing towards a potential role for serum complexation to the *o*BA precursors, leading to the observed slow formation of **14**.

Cumulatively, these results highlight the potential of our platform to give far greater insight into *o*BID chemistry under relevant conditions to their translational applications, and efforts to explore such factors in high throughput are currently underway in our group.

### Alternative *o*BA architectures

The studies described above provided us with detailed insight into the chemistry of the 2-borono-4-alkoxy-benzaldehyde handles that are widely used in the community. However, other handles, most commonly the 3-alkoxy (**22**) and 4-alkyl (**23**) derivatives are also highly relevant. Despite the greatly differing

**Table 2** Tabulated dissociation ( $K_d$ ) and rate ( $k_1$ ,  $k_{-1}$ ) constants for the formation of *o*BIDs **14** and **15** in pH 7.4 PBS in the presence of different additives

	Additive	$k_1/\text{M}^{-1} \text{s}^{-1}$	$k_{-1}/\text{s}^{-1}$	$K_d$
<b>14</b>	—	4370 $\pm$ 164	—	—
<b>14</b>	Glucose	1340 $\pm$ 10	2.04 $\pm$ 0.12 $\times 10^{-4}$	152 nM
<b>14</b>	Fructose	446 $\pm$ 4	2.54 $\pm$ 0.20 $\times 10^{-4}$	571 nM
<b>14</b>	10% Serum	64.0 $\pm$ 4.4	9.03 $\pm$ 2.22 $\times 10^{-4}$	14.1 $\mu$ M
<b>15</b>	—	169 030 $\pm$ 6962	2.60 $\pm$ 0.55 $\times 10^{-6}$	15 pM
<b>15</b>	Glucose	45 750 $\pm$ 6614	2.36 $\pm$ 0.50 $\times 10^{-6}$	51 pM
<b>15</b>	Fructose	16 549 $\pm$ 1338	2.35 $\pm$ 0.50 $\times 10^{-6}$	142 pM
<b>15</b>	10% Serum	153 $\pm$ 6	2.93 $\pm$ 0.20 $\times 10^{-3}$	19.2 $\mu$ M



stereo-electronic configurations of these handles, the effect of this on *o*BID formation has not previously been studied. Basic density functional theory (DFT) calculations suggested that the relative contributions of N–B interactions to *o*BID stability across these analogues, as well as the previously unreported 4-carboxy analogue (**24**), were likely to be significant (up to 30 kJ mol<sup>−1</sup> difference in stabilisation, see ESI Section 14†). Due to the significant synthetic effort needed to derive a series of dye-labelled constructs and controls for each distinct *o*BA, we therefore set out to exploit the data obtained through our FRET study to quantify parameters for each *o*BA in NMR competition studies.

Reactions were run at a 1 : 1 : 1 ratio of 4-alkoxy *o*BA (**25**), *o*BA analogue, and the relevant nucleophile, with product ratios used to determine reaction parameters (Fig. 4). When 1,2-diamine **26** was used as a nucleophile, the rapid equilibration of the system (*i.e.* high  $k_1$  AND  $k_{-1}$ ) allowed us to calculate relative  $K_d$ s, as described in the SI. The results obtained show a clear trend of increasing *o*BID stability as the substituent at the 4-position moved from electron donating (**25**) through to electron withdrawing (**24**). Unfortunately, efforts to perform analogous experiments using a hydrazine nucleophile as a kinetic trap proved unsuccessful, with the rapid rates of reaction leading insufficient resolution to distinguish differences in product distribution.

The intriguing insights provided by these studies of relative *o*BID stability open the door to the design of new *o*BA derivatives with tuneable properties. For example, rational design of highly electron-deficient *o*BA's may lead to the production of *o*BID's with greatly increased stability relative to the current state of the art. Further efforts to explore these possibilities are currently being undertaken.

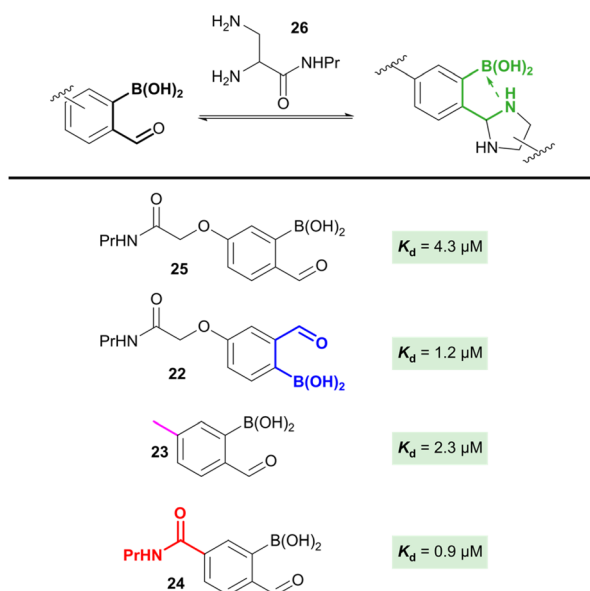


Fig. 4 Competition experiments between 4-alkoxy-*o*BA **25** and analogues **22–24**. A 1 : 1 ratio of **25** and the relevant analogue were combined with 1 equiv. of nucleophile **26** and the product distribution observed by NMR used to calculate  $K_d$ .

## Conclusions

In this study we have developed a novel FRET-based assay that allows the formation of *o*BID's to be probed with unprecedented levels of detail. In particular, the ability to monitor the coupling of *o*BA's and amine-based nucleophiles at low concentrations with high sensitivity provides a direct way to measure conjugation. In turn, this allows us to cumulatively monitor the formation of all species which can contribute to the end applications of *o*BID's, rather than relying on measurements of individual species which may undergo structural exchange and therefore do not represent the full picture.

Using this platform, we were able to calculate  $k_1$ ,  $k_{-1}$ , and  $K_d$  for the most widely used *o*BA-nucleophile pairs used in the literature across a range of conditions, allowing us to identify optimal pH ranges and interesting behaviour that provides new insight into *o*BID chemistry. The ability of our platform to function in the presence of buffer additives is particularly powerful, allowing us to study conjugation chemistry in complex environments such as serum. We therefore provide insight into the rate of formation of *ortho*-borono oximes and hydrazones/DABs for the first time. Our results also suggest that further tuning and optimization of *o*BID chemistry is possible through even small changes to the stereo-electronic configurations of the *o*BA and nucleophile precursors, and our platform provides an ideal means to test such structures. Efforts to do so, and deliver new functional methods relevant to bioconjugation and biomaterials chemistry, are currently underway in our lab, and we hope that our study will serve to stimulate further exploration and optimisation of the underlying chemistry of *o*BID's in the future.

## Data availability

Data associated with the study is available on the University of York Research Database via the <https://doi.org/10.15124/5dfbc414-7af6-4377-9c9f-1ce65103b84e>.

## Author contributions

N. C. R. performed all synthetic studies and FRET measurements, and data analysis and curation. A. V. S. performed preliminary studies which led to this work. E. F. T. performed DFT calculations, supervised by J. M. L., C. D. S. developed the project concept, performed data analysis, supervised and managed the study, and wrote the manuscript. All authors contributed to the editing of the manuscript.

## Conflicts of interest

There are no conflicts to declare.

## Acknowledgements

Prof. Dave Smith and Dr Will Unsworth are thanked for insightful discussions throughout this work. N. C. R. and C. D. S. acknowledge PhD Studentship support from the EPSRC Doctoral Training Partnership and the University of York. A. V.



S. acknowledges support from the Erasmus++ Programme. E. F. T. is grateful to the Royal Society of Chemistry for funding an Undergraduate Research Bursary. DFT calculations were undertaken on the Viking Cluster, which is a high-performance computer facility provided by the University of York. We are grateful for computational support from the University of York High Performance Computing service, Viking and the Research Computing team. J. M. L. is supported through a Royal Society Industrial Fellowship (2022–24). C. D. S. acknowledges support from the Royal Society of Chemistry Research Fund (RF19-8128) and a Royal Society Research Grant (RGS\R1\19120).

## References

- 1 J. P. M. António, J. I. Carvalho, A. S. André, J. N. R. Dias, S. I. Aguiar, H. Faustino, R. M. R. M. Lopes, L. F. Veiros, G. J. L. Bernardes, F. A. Silva and P. M. P. Gois, *Angew. Chem., Int. Ed. Engl.*, 2021, **60**, 25914–25921.
- 2 S. Palvai, J. Bhangu, B. Akgun, C. T. Moody, D. G. Hall and Y. Brudno, *Bioconjugate Chem.*, 2020, **31**, 2288–2292.
- 3 X. Ding, G. Li, P. Zhang, E. Jin, C. Xiao and X. Chen, *Adv. Funct. Mater.*, 2021, **31**, 2011230.
- 4 T. C. French and T. C. Bruice, *Biochem. Biophys. Res. Commun.*, 1964, **15**, 403–408.
- 5 S. Cambray and J. Gao, *Acc. Chem. Res.*, 2018, **51**, 2198–2206.
- 6 S. Chatterjee, E. V. Anslyn and A. Bandyopadhyay, *Chem. Sci.*, 2021, **12**, 1585–1599.
- 7 H. Faustino, M. J. S. A. Silva, L. F. Veiros, G. J. L. Bernardes and P. M. P. Gois, *Chem. Sci.*, 2016, **7**, 5052–5058.
- 8 A. Bandyopadhyay, S. Cambray and J. Gao, *Chem. Sci.*, 2016, **7**, 4589–4593.
- 9 A. Bandyopadhyay and J. Gao, *Chem.–Eur. J.*, 2015, **21**, 14748–14752.
- 10 C. J. Stress, P. J. Schmidt and D. G. Gillingham, *Org. Biomol. Chem.*, 2016, **14**, 5529–5533.
- 11 A. Bandyopadhyay, S. Cambray and J. Gao, *J. Am. Chem. Soc.*, 2017, **139**, 871–878.
- 12 H. Gu, T. I. Chio, Z. Lei, R. J. Staples, J. S. Hirschi and S. Bane, *Org. Biomol. Chem.*, 2017, 7543–7548.
- 13 E. Herbst and D. Shabat, *Org. Biomol. Chem.*, 2016, **14**, 3715–3728.
- 14 P. Schmidt, C. Stress and D. Gillingham, *Chem. Sci.*, 2015, **6**, 3329–3333.
- 15 M. Levitus and S. Ranjit, *Q. Rev. Biophys.*, 2011, **44**, 123–151.
- 16 A. Bandyopadhyay, K. A. McCarthy, M. A. Kelly and J. Gao, *Nat. Commun.*, 2015, **6**, 6561.
- 17 P. M. S. D. Cal, R. F. M. Frade, C. Cordeiro and P. M. P. Gois, *Chem.–Eur. J.*, 2015, **21**, 8182–8187.
- 18 K. Li, C. Weidman and J. Gao, *Org. Lett.*, 2018, **20**, 20–23.
- 19 P. M. S. D. Cal, J. B. Vicente, E. Pires, A. V. Coelho, L. F. Veiros, C. Cordeiro and P. M. P. Gois, *J. Am. Chem. Soc.*, 2012, **134**, 10299–10305.
- 20 O. Dilek, Z. Lei, K. Mukherjee and S. Bane, *Chem. Commun.*, 2015, **51**, 16992–16995.
- 21 D. K. Kölmel and E. T. Kool, *Chem. Rev.*, 2017, **117**, 10358–10376.
- 22 D. Bermejo-Velasco, G. N. Nawale, O. P. Oommen, J. Hilborn and O. P. Varghese, *Chem. Commun.*, 2018, **54**, 12507–12510.
- 23 A. Dirksen, S. Dirksen, T. M. Hackeng and P. E. Dawson, *J. Am. Chem. Soc.*, 2006, **128**, 15602–15603.
- 24 B. Akgun, C. Li, Y. Hao, G. Lambkin, R. Derda and D. G. Hall, *J. Am. Chem. Soc.*, 2017, **139**, 14285–14291.
- 25 G. S. Han and D. W. Domaille, *Org. Biomol. Chem.*, 2021, **19**, 4986–4991.
- 26 X. Wu, Z. Li, X.-X. Chen, J. S. Fossey, T. D. James and Y.-B. Jiang, *Chem. Soc. Rev.*, 2013, **42**, 8032–8048.

